Naval Research Laboratory

Stennis Space Center, MS 39529-5004

NRL/MR/7320--08-9069

Cohesive Sediment Entrainment Rate Functions: Expanding and Quantifying Their Parameterizations

MARK COBB

Planning Systems Incorporated
Stennis Space Center, Mississippi

TIMOTHY R. KEEN

Ocean Dynamics and Prediction Branch
Oceanography Division

April 3, 2008

REPORT DOCUMENTATION PAGE

Form Approved
OMB No. 0704-0188

1. REPORT DATE *(DD-MM-YYYY)*	2. REPORT TYPE	3. DATES COVERED *(From - To)*
03-04-2008	Memorandum Report	

4. TITLE AND SUBTITLE

Cohesive Sediment Entrainment Rate Functions:
Expanding and Quantifying Their Parameterizations

5a. CONTRACT NUMBER

5b. GRANT NUMBER

5c. PROGRAM ELEMENT NUMBER
0601153N

6. AUTHOR(S)

Mark Cobb* and Timothy R. Keen

5d. PROJECT NUMBER

5e. TASK NUMBER

5f. WORK UNIT NUMBER
73-8544-A8-5

7. PERFORMING ORGANIZATION NAME(S) AND ADDRESS(ES)

Naval Research Laboratory
Oceanography Division
Stennis Space Center, MS 39529-5004

8. PERFORMING ORGANIZATION REPORT NUMBER

NRL/MR/7320--08-9069

9. SPONSORING / MONITORING AGENCY NAME(S) AND ADDRESS(ES)

Office of Naval Research
875 North Randolph St.
Arlington, VA 22203-1995

10. SPONSOR / MONITOR'S ACRONYM(S)
ONR

11. SPONSOR / MONITOR'S REPORT NUMBER(S)

12. DISTRIBUTION / AVAILABILITY STATEMENT

Approved for public release; distribution is unlimited.

13. SUPPLEMENTARY NOTES

*Planning Systems Inc., Stennis Space Center, MS 39529
(Formerly of the Ocean Dynamics and Predictions Branch, Oceanography Division, Stennis Space Center, MS)

14. ABSTRACT

The erosion characteristics of cohesive sediments in nearshore environments depend on a number of biogeochemical processes. It is standard practice to experimentally determine the entrainment rate of sediment into the water column as a function of the applied bottom shear stress and fit this data to a power law function. This work addresses the inherent problems of fitting entrainment rate data to parameterized functions, focusing on the non-uniqueness of the power law approach and its sensitivity to errors in the data. An approach for incorporating the effects of bioturbation and consolidation, thus expanding the parameter space of the entrainment function, into the standard power law formulation is examined with regard to its physical sensitivity and its expanded predictive capability of biogeochemical changes in cohesive sediments. Finally, power law and exponential entrainment functions are compared in order to illustrate the physical sensitivity of a particular entrainment parameterization.

15. SUBJECT TERMS

Entrainment function	Cohesive sediments	Bioturbation
Parameterization	Erosion	Consolidation

16. SECURITY CLASSIFICATION OF:			17. LIMITATION OF ABSTRACT	18. NUMBER OF PAGES	19a. NAME OF RESPONSIBLE PERSON
a. REPORT	b. ABSTRACT	c. THIS PAGE			Timothy Keen
Unclassified	Unclassified	Unclassified	UL	35	19b. TELEPHONE NUMBER *(include area code)* (228) 688-4950

CONTENTS

1. Introduction

The transport of cohesive sediments in nearshore environments such as bays and estuaries presents significant challenges to the modeling community (Violeau et al. 2002). Predicting the movement of sediment and pollutants in estuaries and at the mouths of rivers under a variety of conditions is a long-term goal of sediment transport modeling. Because cohesive sediments can remain suspended for long durations, they can be transported great distances by currents and significantly affect the nearshore environment. In particular, they can reduce the water clarity and transport pollutants far from their point of origin (Mehta 1989a). In order to better manage coastal regions, it is necessary to understand the physical and biological processes (i.e. mineralogy, salinity, organic carbon content, bioturbation) that affect the entrainment of cohesive sediments and incorporate them into predictive models. The endeavor of creating realistic models for cohesive sediment transport requires a large-scale community effort to understand the physics of these sediments and the environments in which they are created. This work examines one approach to this problem and the inherent problems of increasing the complexity of entrainment functions typically applied to cohesive sediment transport. The goal of this work is to illustrate a general methodology (not an overall solution) and how it can lead to more robust cohesive sediment entrainment functions.

The sediments in coastal environments experience forces generated by wave, wind, and tidal action (Dronkers and Miltenburg 1996). Sediments are suspended by turbulence within the bottom boundary layer and are transported by the mean flow, eventually settling out of suspension. These physical processes are not well understood and are currently areas of intense research in the scientific and engineering communities.

Manuscript approved March 31, 2008.

Consequently, realistic coupled model systems to describe these environments are only now being developed (Bruens et al. 2002, Peterson and Vested 2002, Schweim et al. 2002). In addition, and of equal importance, biogeochemical processes, flocculation, and consolidation occur in the water column and within seafloor sediments. These processes determine the material properties of the sediments at the water-sediment interface and thus determine their entrainment properties (Mehta et al. 1989b). The influence of biological and physical processes on mudflats has been examined in the INTRMUD project (Black et al., 1998), which demonstrated the importance of biostabilization on entrainment (de Brouwer et al., 2000; Droppo et al. 2001). The LISP project (Littoral Investigation of Sediment Properties) (Daborn, 1991) also examined the complex interaction of microflora and fauna in the intertidal environment. The biostabilization effect of biofilms is opposed by the destabilization caused by bioturbation (Grant and Daborn, 1994; Green et al., 2002). Laboratory work with natural sediments has shown that cohesive sediment erodibility increases rapidly with the activity of infauna, presumably because of their destruction of inter-particle bonds and primary depositional fabric (Tsai and Lick, 1988; Lintern et al., 2002). The complex interaction of these biological processes with physical processes like hydrodynamics and consolidation necessitates the use of more realistic entrainment models and carefully planned measurement programs (Tolhurst et al., 2000; Lick et al., 1998).

It is therefore necessary to quantify the effects that the pre- and post-depositional environments have on the physical properties of the sediments and incorporate these characteristics into predictive models through an entrainment function. The goal of this work is to demonstrate that one common approach to parameterizing entrainment

functions is not sufficiently robust to capture the complex processes that determine how cohesive sediments erode in nearshore environments. The broad spectrum of biogeochemical processes that occur within marine sediments require that entrainment functions be enhanced with more degrees of freedom to account for the complex time-dependent entrainment characteristics of marine sediments. In lieu of first-principles models that can predict the microscopic properties of cohesive sediments an empirical fitting procedure is still necessary, but such an approach must account for a broad range of sediment characteristics and how they evolve after deposition. Once again we emphasize that this is an example of a new kind of methodology for approaching entrainment functions rather than an overall solution to this very complex problem.

Power law parameterizations (e.g. Kandiah 1974, Lavelle et al. 1984, Lick et al. 1995) of the entrainment rate will be investigated in order to demonstrate the inherent problems of using entrainment functions with small parameter spaces. In particular, the non-uniqueness of this formulation and the problems of fitting it to data will be discussed. An approach that incorporates the effects of bioturbation and consolidation into the entrainment rate function will be examined as well (Keen and Furukawa 2006, hereinafter KF06). The KF06 approach for parameterizing the entrainment rate function demonstrates that more physical models of entrainment rate parameters can be developed for marine sediments. Such an approach provides the entrainment function with a certain degree of sensitivity to the physical environment and post-depositional evolution of the sediments which can only be improved through better models of the sediment physiochemical properties. We will also address the issue of different entrainment

parameterizations as well as the development of more fundamental models for cohesive sediment entrainment.

2. Fundamental Entrainment Rate Formulation

Commonly used power law formulations for the entrainment or erosion rate (kg m^{-2} s^{-1}) of cohesive sediments are typically expressed in terms of an erosion constant and the critical shear stress. For this work we refer to entrainment rate functions that have the general form:

$$E_B = A_0 \left(\frac{\tau}{\tau_c} - 1 \right)^m = A_0 \left(\tau^* \right)^m \quad (1)$$

where τ_c, A_0, m are empirically determined constants (Lick et al. 1995); A_0 has units of kg m^{-2} s^{-1}; τ and τ_c (Pa) are, respectively, the bottom shear stress and the critical shear stress at which entrainment occurs. The excess shear stress, given by the term in parentheses, is represented by τ^*. Equation (1) expresses the dependence of the sediments on the excess shear stress as well as the intrinsic entrainment properties of the material through the coefficient A_0. In principle, τ_c, A_0, and m should be functions of sediment properties such as water content, time since deposition, bioturbation, organic content, mineralogy, salinity, and floc size (see Partheniades 1986, for a review of the mechanical and chemical properties of bottom sediments and their effects on erosion). However, these dependencies are not explicitly treated in Equation (1). In some cases, the critical shear stress is given a dependency on depth below the seafloor because it is known to increase with consolidation and dewatering (Mehta et al., 1989b). A standard procedure for

determining the parameters τ_c, A_0, and m for a particular sediment sample is to fit Equation (1) to the entrainment rate data as a function of the applied shear stress (Lick et al. 1995). Because the dimensionless power m is determined by fitting Equation (1) to a particular data set its relationship to the sediment properties (and thus τ_c and A_0) is poorly understood and lacks a physically intuitive basis for its value (Lick et al., 1995). Unfortunately, as will be discussed further, the fitting procedure ignores the physical relationships that must certainly exist between these parameters and essentially lumps much of the sediment's physical complexity into the erosion constant and critical shear stress parameters. It is the conclusion of this study that such an approach is simply too limited in its formulation for realistic sediments that are subjected to a variety of time-dependent physical and biogeochemical processes.

To illustrate the essential problem of fitting field measurements to power laws we examine the non-uniqueness of Equation (1), which can be rewritten as

$$\tau^* = e^{\frac{-\ln(\frac{A_0}{E_B})}{m}} = \left(\frac{A_0}{E_B}\right)^{-\frac{1}{m}} \tag{2}$$

Using this formulation, a surface of constant entrainment rate (Figure 1) can be plotted to demonstrate that there are an infinite number of possibilities for the parameters τ^*, A_0, and m (assuming that τ^* and A_0 are always positive) for a specified value of the entrainment rate (E_B = 0.1 kg m^{-2} s^{-1}). The ranges of the x and y axes were chosen to coincide with values of A_0 and m that are reasonable for fitting known data sets (KF06). From the analysis of several data sets in KF06 it is clear that A_0 can vary over several orders of magnitude and that m will be on the order of ~1 to 3. For E_B equal to 0.1 kg m^{-2}

s^{-1}, τ^* is observed to decrease with increasing values of both A_0 and m. Figure 1 demonstrates that it is possible to have sediments with very different physical properties eroding at the same rate, even if they are from the same sample suite, and indicates that Equation (1) should be used with caution when analyzing entrainment data. If it is assumed that both τ and τ_c vary spatially and temporally during an experiment (Parchure and Mehta 1985), then it is conceivable that A_0 and m are also changing in space and time. Therefore if τ^*, A_0, and m are assumed to be dependent not only on the sediment properties but also on each other, a much more complex and robust entrainment rate function can be derived.

Figure 1 indicates that τ^* decreases with increasing A_0 and m, although this is only for a small range of the potential values for A_0 and m. Figure 2 is a two-dimensional projection of the isosurface plotted in Figure 1, but for a different range of A_0. The same value of the entrainment rate (E_B = 0.1 kg m^{-2} s^{-1}) is used for Figures 1 and 2. For A_0 greater than E_B, τ^* increases with increasing m for a constant value of A_0, whereas τ^* decreases with increasing m for constant A_0 less than E_B. Specifically, the contours of τ^* change direction when the natural log of A_0/E_B changes sign, as indicated by Equation (2). This transition can be observed as A_0 becomes greater then 0.1 kg m^{-2} s^{-1} and the contour lines of τ^* change from having negative slopes in the direction of increasing m to having positive slopes. The transition will always occur along the contour $\tau^* = 1.0$ because the natural log of (A_0/E_B) is zero at the transition. This behavior is not unexpected from a mathematical point of view since A_0 and m must adjust along a τ^* isocontour if E_B is being held constant, but this sensitivity has not been addressed in the literature. Therefore, when experimental data are used to estimate the values of the

parameters in Equation (1), the range of A_0 and m should be considered because it may have a significant impact on the results. In particular, uncertainties in observations of entrainment rate and excess shear stress can lead to different results for A_0 and m, depending on how these quantities are related in the particular region of parameter space encompassed by the experiments. Additional constituent equations relating these parameters to the physical properties of the sediments as well as each other would make the solution procedure more complex but would nevertheless provide more physical constraints on how each parameter should vary.

Another way of viewing the sensitivity of the entrainment rate to τ^*, A_0, and m is to examine its behavior when τ^* is held constant. Assuming a constant τ^* equal to 9.0, A_0 and m can have a range of values along an isocontour of the entrainment rate E_B (Figure 3). The contours of constant entrainment rate are plotted in Figure 4, which is a two dimensional projection of Figure 3. It can be seen from Figures 3 and 4 that E_B increases with increasing A_0 and m as expected for τ^* greater than 1. However, when τ^* is less than 1, the contours have a very different structure (Figure 5). The isolines of E_B in Figure 4 are essentially orthogonal to those of Figure 5, indicating a significant change in the parameter space for τ^* less then 1. These examples demonstrate that sediment samples with uniform excess shear stress and constant entrainment rates do not necessarily have to have uniform physical properties. Overall Figures 1-5 illustrate how insensitive Equation (1) is to the actual physical properties of the sediments and motivate a parameterization strategy that incorporates additional physics into the entrainment function.

Before discussing extensions to Equation (1), it is useful to examine representative surfaces of constant E_B in (τ^*, A_0, m) parameter space (Figure 6). If Equation (1) is fit to a set of experimental data points, the resulting constant values of A_0 and m represent a vertical line parallel to the τ^* axis. This line intersects surfaces of constant entrainment rate measured for different values of excess shear stress. This is demonstrated in Figure 6 using isosurfaces of E_B equal to 0.1 kg m^{-2} s^{-1} (lower surface) and 0.5 kg m^{-2} s^{-1} (upper surface). Planes of constant τ^* intersect these E_B isosurfaces along curved lines. Thus there are an infinite number of values for A_0 and m, along each curve of constant τ^*, for each E_B isosurface (as seen previously in Figure 2). Furthermore, measurement uncertainties in the entrainment rate and excess shear stress can produce very different values of A_0 and m, depending on the geometry of the E_B isosurface. Measurement errors in τ^* are more important in determining A_0 and m if the E_B isosurface is slowly changing in parameter space. This is because small variations in τ^* represent large changes in the values of A_0 and m if the E_B isosurface varies slowly over a large area of the A_0-m plane. As seen from Figure 6, different E_B isosurfaces can have very different gradients in parameter space with respect to how τ^* changes with A_0 and m. A more realistic model would allow A_0 and m to vary along the τ^* contours of each E_B isosurface while still satisfying Equation (1) for each (E_B, τ^*) data point. This would be an important step in going beyond the standard curve fitting procedures that are used in the literature. In addition, such an approach would increase the correlation of A_0 and m with the physical properties of the sediments.

3. Entrainment Rate Formulation with Bioturbation and Consolidation

Natural sediments experience a complex physical and biogeochemical environment, which affects their physical properties and thus the manner in which they erode. The previous section demonstrated that a simple parameterization of cohesive sediment entrainment rate such as Equation (1) does not have the capacity to describe the spatial and temporal changes that occur in the erosion characteristics of natural sediments in a robust manner. An initial approach for extending the entrainment rate function (KF06) incorporates physical and biological effects into the entrainment coefficient A_0 of Equation (1). The A_0 parameter can be expanded into three coefficients $A_0A_BA_C$, in which A_0 represents an entrainment parameter fundamental to a particular sediment type (i.e. the mineralogy), A_B represents the effects of bioturbation, and A_C represents the effects of consolidation.

In the KF06 study the consolidation factor was fit to an exponential function,

$$A_C = C_1 e^{(W-W_o)/t_1} \tag{3}$$

where: $C_1 = 3.97\text{x}10^{-3}$, $t_1 = 1.99315$, W is the water content (%) of the sediment, and $W_0 = 62.85$. The values of C_1, t_1, and W_0 were derived by fitting Equation (3) to consolidated sediments from Lake Erie with no bioturbation (Fukuda and Lick 1980). Equation (3) is only valid for W ranging from 61.5 to 74% since this was the range of the water content data used to determine the parameters. It is apparent from Equation (3) that a decrease in W corresponds to increased consolidation and a lower entrainment rate. This parameterization is therefore expressing the physical effects of consolidation on the entrainment rate. The bioturbation factor is fit to a parabolic function of time,

$$A_B = C_2 + C_3 t + C_4 t^2 \tag{4}$$

where: C_2 = 5.093x10^{-3} and C_3 = 2.186x10^{-2} (day^{-1}) and C_4 = 6.85x10^{-4} (day^{-2}). The values of C_2, C_3, and C_4 are found by fitting Equation (4) to entrainment data for bioturbated sediments from the Tamar Estuary in the United Kingdom (Lintern et al. 2002). The interval of time over which bioturbation occurs is t, often interpreted as the time since deposition, and it is apparent from Equation (4) that the entrainment rate should increase with t. Equation (4) therefore incorporates the physical changes in the sediments (i.e. weakening of physical integrity) due to bioturbation. The methods and data used to derive the parameters A_B and A_C are discussed in detail in KF06. Note that the A_B and A_C parameters are dimensionless quantities. The expanded form of the entrainment rate function is

$$E_B = A_0 A_B A_C \left(\frac{\tau}{\tau_c} - 1 \right)^m \tag{5}$$

At this point we can focus on the sensitivity of the entrainment rate function to the parameters A_B and A_C as well as time since deposition t and water content W. It is the functional dependence of A_B and A_C on measurable physical quantities that leads to a more robust and realistic model of the entrainment rate. Although we are still using functions that have been fitted to a limited set of data they can describe a broader range of sediment entrainment properties. A much broader data base of sediment entrainment

measurements for a variety of different types of sediments is required for more generality and perhaps different functions for different ranges of water content and deposition time are required as well. The discussion in section (1) regarding the general properties of the parameter space for Equation (1) applies equally to Equation (5) and will not be repeated here.

The entrainment rate computed from Equation (5) is plotted as a function of both time and water content in Figures 7 and 8, respectively, in order to show the relative effects (i.e. magnitude) of bioturbation and consolidation. The ranges of t and W are similar to those used in KF06 to obtain the original parameterizations of A_B and A_C. The values of A_0 and τ^* are set equal to 1 and $m = 0$ so that the curves in Figures 7 and 8 are equal to the values of A_B and A_C respectively. The entrainment rate is much more sensitive to small changes in water content due to the exponential form of A_C then it is to deposition time (and hence bioturbation). It takes approximately 25 days for E_B to equal 1 kg m^{-2} s^{-1} in Figure 7 whereas a change of 4% in the water content (Figure 8) results in an equivalent change in the value of E_B. A contour plot of entrainment rate E_B as a function of time since deposition and water content (Figure 9), with A_0 and τ^* equal to 1.0, can be interpreted as representing the product $A_B A_C$. The conclusion to be drawn from Figure 9 is that sediments should be characterized with regard to their physical properties and post-depositional histories and not just their entrainment at different shear stress values. It is evident from Figure 9 that the same entrainment rate can be obtained for very different consolidation and bioturbation values and thus a prediction of the entrainment rate will depend on understanding the sediment properties and the environments in which they form. Increasing the sensitivity of entrainment functions to the material properties

of sediments therefore requires a deeper understanding of how sediments form and change in nearshore environments.

Perhaps the most direct way of comparing the relative effects of consolidation and bioturbation is to determine the entrainment rate as a function of excess shear stress with either bioturbation or consolidation affecting the sediment's erosion properties (Lavelle et al. 1984). Figure 10 plots the entrainment rate calculated from Equation (5) against excess shear stress with either bioturbation or consolidation activated. The deposition time of 5 days and water content of 70% are chosen to produce similar curves over a range of shear stress values with A_0 = 0.001 kg m^{-2} s^{-1} and m = 2.5. This leads again to the problem suggested by figure 9 of how to predict the entrainment rate if bioturbation and consolidation are both affecting the sediment properties. Both processes are present in natural sediments but it is often unclear what their individual contributions are to determining the properties of the bed.

Although the entrainment rate determined from Equation (5) depends on the post-depositional history through A_B and A_C there is still much more that could be done with respect to how *their* parameters evolve with time. This is a much larger issue which must eventually be addressed if robust predictive models of cohesive sediment transport are to be developed for nearshore environments. Although an approach similar to that employed in this paper for A_B and A_C could be used to create additional functional parameterizations, assuming that the data exists to construct such functions. This problem can be dealt with to some extent by adjusting A_0, but this requires an *ad hoc* (and unphysical) change in a fundamental parameter. The implicit problem with natural sediments is that both consolidation and bioturbation processes are time-dependent. In

addition, the final state of a sediment sample is dependent not only on its depositional history but also on its initial state with respect to infauna and water content. This discrepancy can only be addressed by more realistic models as well as more extensive field studies of natural marine sediments.

4. Comparison of Power Law and Exponential Models of Entrainment Rate

The parameterizations included in Equation (1) and its extended version, Equation (5), have been examined in order to show their potential as well as their limitations. The limitations of Equation (1) with respect to the depth dependence of flocculated sediment have been discussed by Parchure and Mehta (1985). They found it difficult to fit their entrainment data to a power law such as Equation (1) and instead used an exponential function of shear stress with a depth-dependent critical shear stress τ_c. This section compares Equation (1) to an exponential entrainment rate function in order to address the need for physical correlations between the various parameters of any proposed entrainment function.

The exponential entrainment rate function employed for this discussion has the following form:

$$E_B = \varepsilon_0 e^{\tau/\alpha} \tag{6}$$

where: ε_0 (kg m^{-2} s^{-1}) is the fundamental entrainment coefficient; τ is the bottom shear stress; and α is a parameter with units of shear stress. The entrainment rates calculated from Equations (1) and (6) are compared in Figure 11, which plots both as functions of

the shear stress τ. The curves are obtained by setting A_0 and ε_0 equal to 1 kg m^{-2} s^{-1} and adjusting the other parameters as needed. For the power law function, the m exponent is 2.4 and τ_c is 0.05 Pa whereas the value of α is 0.1 Pa for the exponential function. It should be noted that the values of entrainment rate in Figure 11 are not representative of actual field results and that both functions would have to be scaled down by lowering the values of A_0 and ε_0. It should also be pointed out that Equation (6) only applies to τ greater than τ_c. Equation (6) never goes to zero unlike Equation (1) which is equal to zero when τ equals τ_c. The two curves have approximately the same magnitude over a small range of τ, with the exponential entrainment exceeding the power law entrainment when τ becomes greater than 0.55 Pa.

The fact that the two curves are similar over a narrow range of values is significant with regard to modeling entrainment. What physical significance do these parameters actually have if it is possible to make Equations (1) and (6) agree over some range of shear stress by simply adjusting their values? These adjustments must be arbitrarily determined because the parameters of each entrainment function are not correlated with each other in any physical way. This demonstrates the lack of any physical basis for the parameterizations of Equations (1) and (6) and further supports the need for empirically derived constitutive equations that govern the relationships between the parameters of an entrainment function.

5. Discussion

The increased parameterization of A_0 presented in section 3 is intended to introduce more physical sensitivity to this parameter, although Equations (3) and (4) are still

limited by their lack of dynamical feedback with the local sedimentary environment. Because the water content and bioturbation parameters were determined using entrainment data dominated by those individual processes and not through dynamic models, it is impossible to gauge whether A_B or A_C is the dominant factor in the erosion of real cohesive sediments when both processes occur simultaneously. This would require the development of a coupled water column–seafloor benthic boundary layer model that could predict deposition, erosion, bioturbation, and consolidation, as well as their cumulative effects on sediment water content and structural properties (Kranenburg and Winterwerp 1997, Petersen and Vested 2002). A discussion of such models is beyond the scope of this paper, although they are the next logical step in cohesive sediment transport modeling.

As demonstrated by Figure 11 fitting parameterized functions to data is a non-trivial matter since the physical interpretation of their parameters can be uncertain. It is necessary to determine the physical or biological processes of most interest *a priori* and select a model that is based on them or neglect physical interpretations entirely. Furthermore, increasing the number of non-physical parameters (i.e. those with no direct physical interpretation) used in the entrainment function decreases its overall sensitivity to physical changes in the sediments. The m exponent in Equation (1) is a good example of a non-physical parameter. It is a non-dimensional number that will change based on some physical properties of the sediments, yet a physical interpretation of m with respect to sediment properties has not been explicitly discussed in the literature to the authors' knowledge.

6. Conclusion

The issues addressed in this work demonstrate the need for physics based approaches to cohesive sediment transport. As demonstrated in this study, power law entrainment rate functions do not have the ability to represent the broad range of erosion characteristics found in nearshore cohesive sediments. In order to model the erosion, transport, and deposition of cohesive sediments in a robust and realistic manner, the physical and biogeochemical processes that determine their physical properties must be understood at a more fundamental level.

The non-uniqueness of a power law entrainment rate function has been examined in order to demonstrate the inherent problems with fitting such functions to entrainment rate data. The results of this analysis clearly show that an isosurface of the entrainment rate could have an infinite number of possible values for A_0 and m and still represent a single data point of (E_B, τ^*). This suggests that sediment properties can vary significantly in time and space and that fitting entrainment rate functions to only certain types of data may simply be ignoring the complex erosion characteristics of the sediment. In addition it also suggests that the parameters determined from one set of data may not be applicable to another set of data (taken at a different time or location). Furthermore, an analysis of multiple surfaces of entrainment rate indicates how restrictive the parameter fitting is with regard to the range of possible parameter values. These results demonstrate the need for entrainment rate functions that incorporate effects such as bioturbation and consolidation.

One approach for extending entrainment rate functions involves using measurable sediment properties such as water content and bioturbation to parameterize the

fundamental entrainment coefficient A_0. As discussed in this work, the entrainment coefficient A_0 can be expanded into sub-coefficients (i.e., $A_0A_BA_C$) that are fitted to data that represent the effects of either bioturbation or consolidation on the sediment sample. Although such an approach is limited by the data sets that are used as well as the inability of the fitted functions to respond dynamically to changing environmental conditions it is a step forward in making entrainment functions more physically realistic. The overall conclusion is that more fundamental and comprehensive coupled models of the water column-sea floor benthic boundary layer should be developed to predict sediment erosion and transport in complex nearshore environments.

Finally, a comparison of power law and exponential entrainment rate functions was performed in order to demonstrate the necessity for physics based parameterization schemes. It was found that different entrainment rate functions can have similar magnitudes over the same range of shear stress values if the parameters of each function are adjusted accordingly. This analysis demonstrated that the physical characteristics of the sediments are not well represented by arbitrary parameterizations (the general theme of this work) and that additional constitutive equations (derived from first principle models or empirical field data) are necessary to create physics based entrainment functions.

7. Acknowledgements

The authors would like to acknowledge Yoko Furukawa and Nathaniel Plant at code 7400 of the Naval Research Laboratory, Stennis Space Center, MS, 39529 for interesting discussions pertaining to sediment transport and the benthic boundary layer. This work is funded by the Office of Naval Research (Program Element 61153N).

8. References

Black, K.S., Paterson, D.M., and Cramp, A. (eds.), 1998, *Sedimentary Processes in the Intertidal Zone. Geological Society of London, Special Publication*, 139.

Bruens, A. W., Kranenburg, C., and Winterwerp, J. C. (2002). "Physical modeling of entrainment by a Concentrated Benthic Suspension." *Fine Sediment Dynamics in the Marine Environment*, edited by J.C. Winterwerp and C. Kranenburg, pp. 109-124, Elsevier, New York.

Daborn, G. R. (ed.), 1991, Littoral investigation of sediment properties, Final Report. Acadia Centre for Estuarine Research, Publication No. 17, 239 pp.

de Brouwer, J.F.C., Bjelic, S., de Deckere, E.M.G.T., and Stal, L.J., 2000, Interplay between biology and sedimentology in a mudflat (Biezelingse Ham, Westerschelde, The Netherlands), *Continental Shelf Research*, 20, 1159-1177.

Dronkers, J., and Miltenburg, A. G. (1996). "Fine sediment deposits in shelf seas." *J. Marine Systems, 7*, 119-131.

Droppo, I.G., Lau, Y.L., and Mitchell, C., 2001, The effect of depositional history on contaminated bed stability, *Science of the Total Environment*, 266 (1-3), 7-13.

Fukuda, M. K., and Lick, W. (1980). "The entrainment of cohesive sediments in freshwater." *J. Geophys. Res., (85)*, 2813-2824.

Grant, J. and Daborn, G., 1994, The effects of bioturbation on sediment transport on an intertidal mudflat, *Netherlands Journal of Sea Research*, 32 (1), 63-72.

Green, M.A., Aller, A.C., Cochran, J.K., Lee, C., and Aller, J.Y., 2002, Bioturbation in shelf/slope sediments off Cape Hatteras, North Carolina: The use of TH-234, Ch1-a, and Br- to evaluate rates of particle and solute transport, *Deep-Sea Research Part II – Topical Studies in Oceanography*, 49 (20), 4627-4644.

Kandiah, A. (1974). "Fundamental aspects of surface erosion of cohesive soils." Ph.D. thesis, Univ. of Calif., Davis.

Keen, T. R., and Furukawa, Y. (2006). "A Modular Entrainment Model for Cohesive Sediment." *Proceedings of the international conference on cohesive sediment Modeling: INTERCOH 2003*, pp. 184-202.

Kranenburg, C., and Winterwerp, J. C. (1997). "Erosion of Fluid Mud Layers. I: Entrainment Model." *J. of Hydraul. Eng., 123(6)*, 504-511.

Lavelle, J. W., Mofjeld, H. O., and Baker, E. T. (1984). "An In Situ Erosion Rate for a Fine-Grained Marine Sediment." *J. Geophys. Res., 89(4),* 6543-6552.

Lick, W., Chroneer, Z., Jones, C., and Jepsen, R., 1998, A predictive model of sediment transport, in *Proceedings, Fifth International Conference, Estuarine and Coastal Modeling*, ASCE., Reston, Virginia, 389-399.

Lick, W., Xu, Y. J., and McNeil, J. (1995). "Resuspension Properties of Sediments from the Fox, Saginaw, and Buffalo Rivers." *J. Great Lakes Res., 21(2)*, 257-274.

Lintern, D.G., Sills, G. C., Feates, N., and Roberts, W. (2002). "Erosion properties of mud beds deposited in laboratory settling columns." *Fine Sediment Dynamics in the Marine Environment*, edited by J.C. Winterwerp and C. Kranenburg, pp. 343-357, Elsevier, New York.

Mehta, Ashish J. (1989a). "On estuarine cohesive sediment suspension behavior." *J.*

Geophys. Res., 94(10), 14,303-14,314.

Mehta, Ashish J., Hayter, E. J., Reginald, W., Krone, R. B., and Teeter, A. M. (1989b). "Cohesive Sediment Transport I: Process Description." *J. of Hydraul. Eng., 115(8)*, 1076-1093.

Parchure, T. M., and Mehta, A. J. (1985). "Erosion of Soft Cohesive Sediment Deposits." *J. of Hydraul. Eng., 111(10)*, 1308-1326.

Partheniades, E. (1986). "A Fundamental Framework for Cohesive Sediment Dynamics." *Estuarine Cohesive Sediment Dynamics: proceedings of a workshop on cohesive sediment dynamics with special reference to physical processes in estuaries*, edited by Ashish J. Mehta, pp. 219-250, Springer-Verlag, New York.

Petersen, O., and Vested, H. J. (2002). "Description of Vertical exchange processes in numerical mud transport modeling." *Fine Sediment Dynamics in the Marine Environment*, edited by J.C. Winterwerp and C. Kranenburg, pp. 375-391, Elsevier, New York.

Schweim, C., Prochnow, J. V., and Köngeter, J. (2002). "Numerical Assessment of Source and Sink Terms for Cohesive Sediments." *Fine Sediment Dynamics in the Marine Environment*, edited by J.C. Winterwerp and C. Kranenburg, pp. 671-685, Elsevier, New York.

Tolhurst, T.J., Riethmuller, R., Paterson, D.M., 2000, In situ versus laboratory analysis of sediment stability from intertidal mudflats, *Continental Shelf Research*, 20, 1317-1334.

Tsai, C. H. and Lick, W., 1988, Resuspension of sediments from Long Island Sound (U.S.A.), *Water Science Technology*, (20) 6/7, 155-164.

Violeau, D., Bourban, S., Cheviet, C., Markofsky, M., Petersen, O., Roberts, W., Spearman, J., Toorman, E., Vested, H. J., and Weilbeer, H. (2002). "Numerical simulation of cohesive sediment transport: intercomparison of several numerical models." *Fine Sediment Dynamics in the Marine Environment*, edited by J.C. Winterwerp and C. Kranenburg, pp. 75-89, Elsevier, New York.

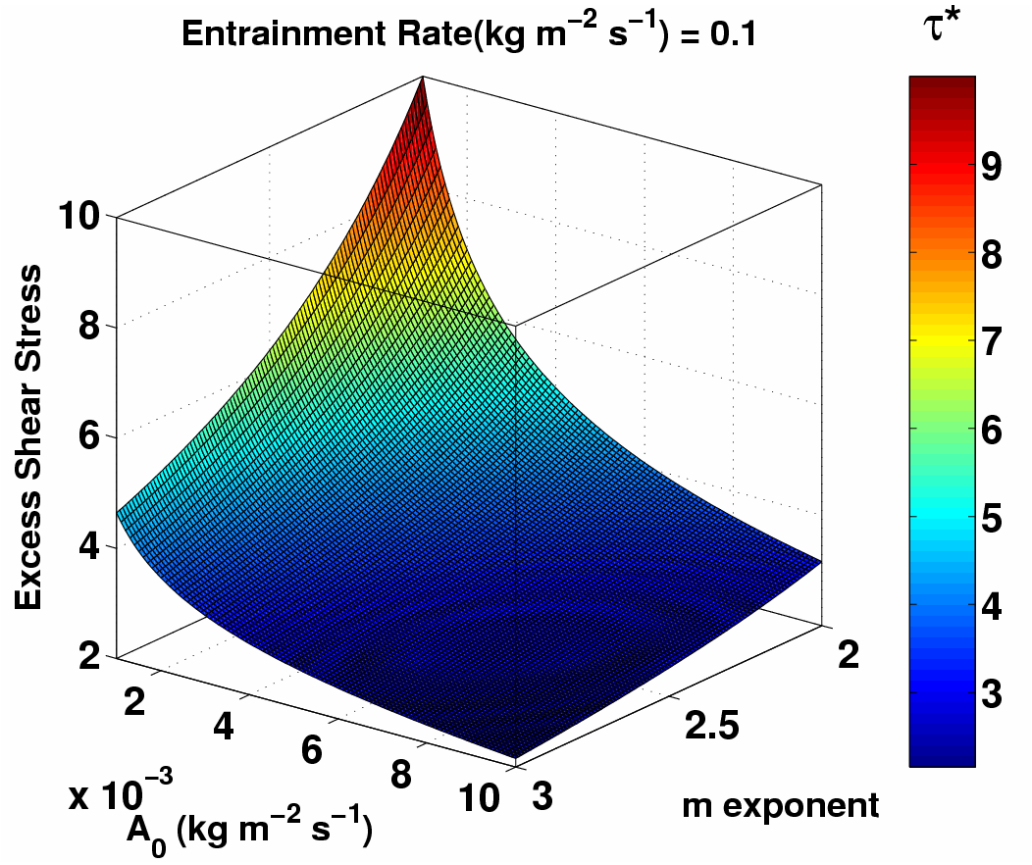

Figure 1. Isosurface of constant entrainment rate (E_B = 0.1 kg m^{-2} s^{-1} for a range of τ*, A_0, and m).

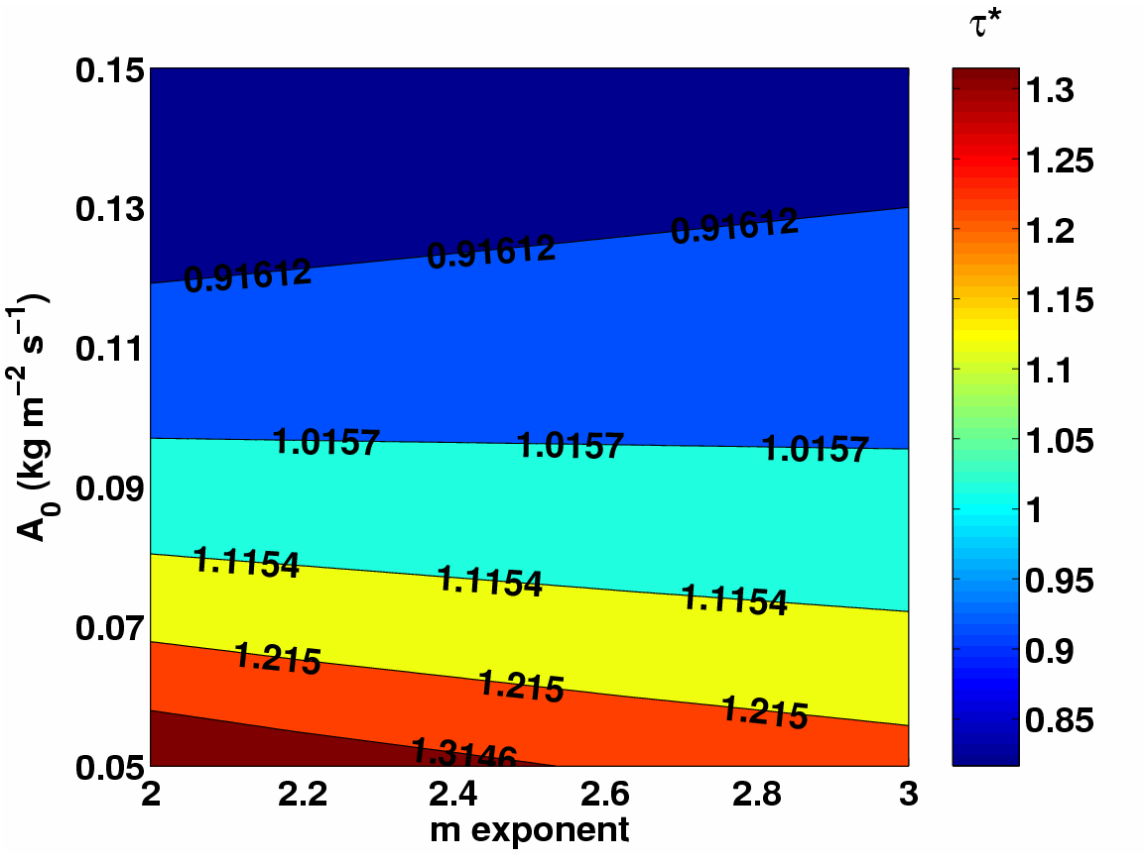

Figure.2. Contour plot of τ^* as a function of A_0 and m for E_B = 0.1 kg m^{-2} s^{-1}.

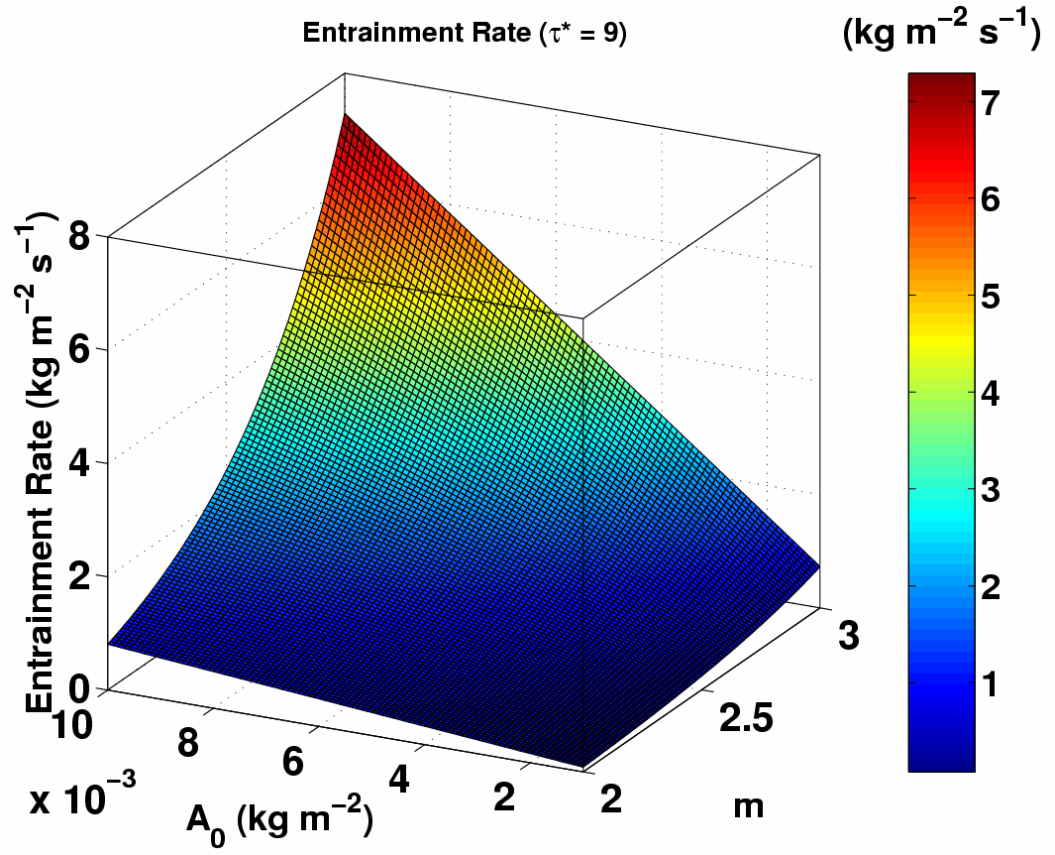

Figure 3. E_B (kg m^{-2} s^{-1}) as a function of A_0 and m for a constant value of $\tau^* = 9.0$.

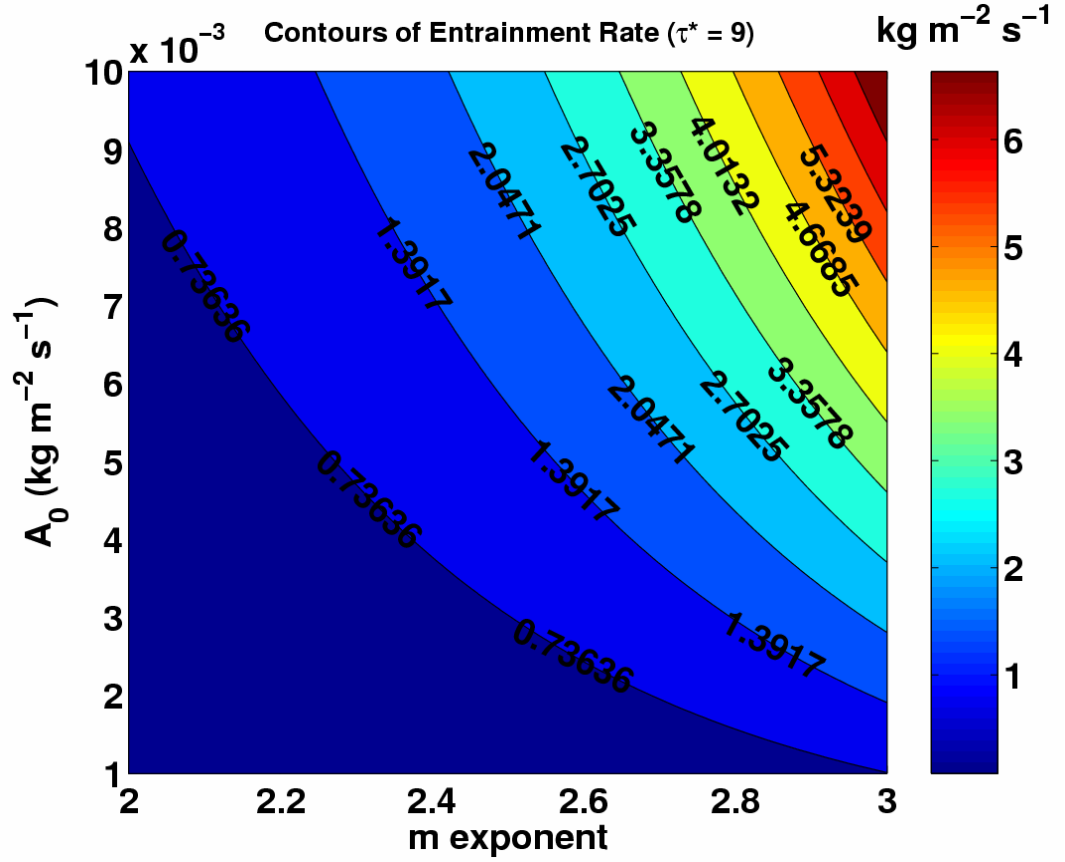

Figure 4. Contour plot of E_B (kg m^{-2} s^{-1}) as a function of A_0 and m for $\tau^* = 9.0$.

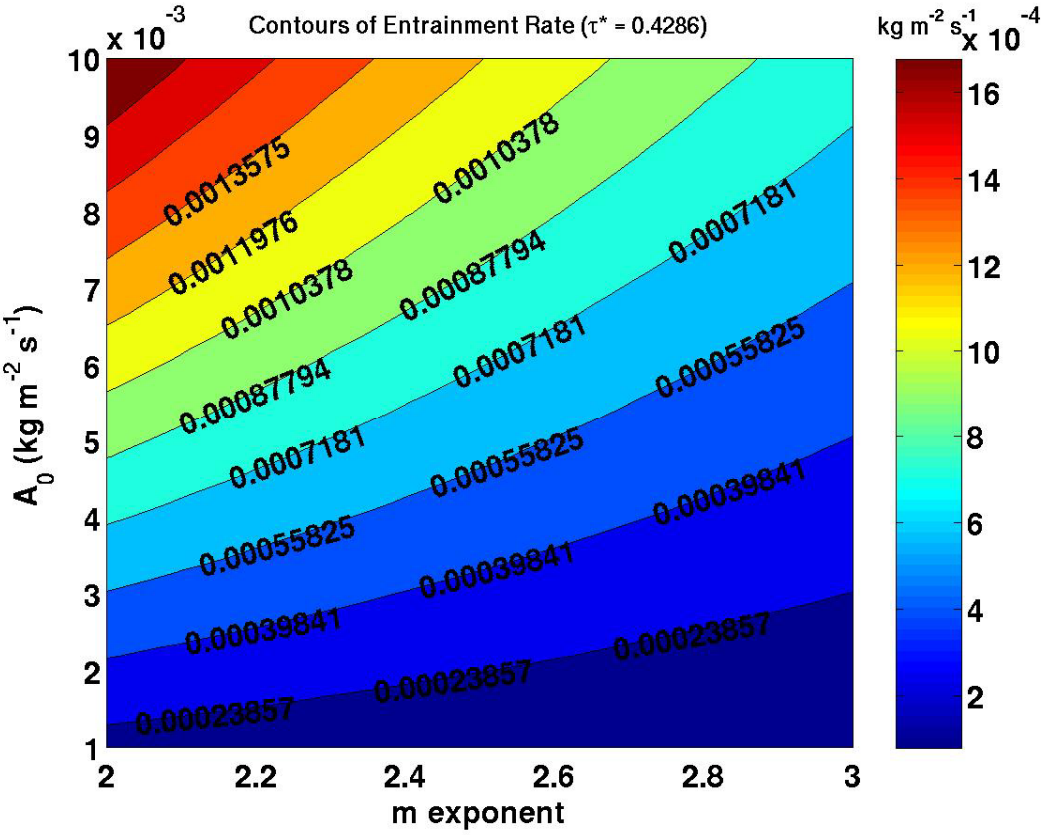

Figure 5. Contour plot of E_B (kg m^{-2} s^{-1}) as a function of A_0 and m for $\tau^* = 0.4286$.

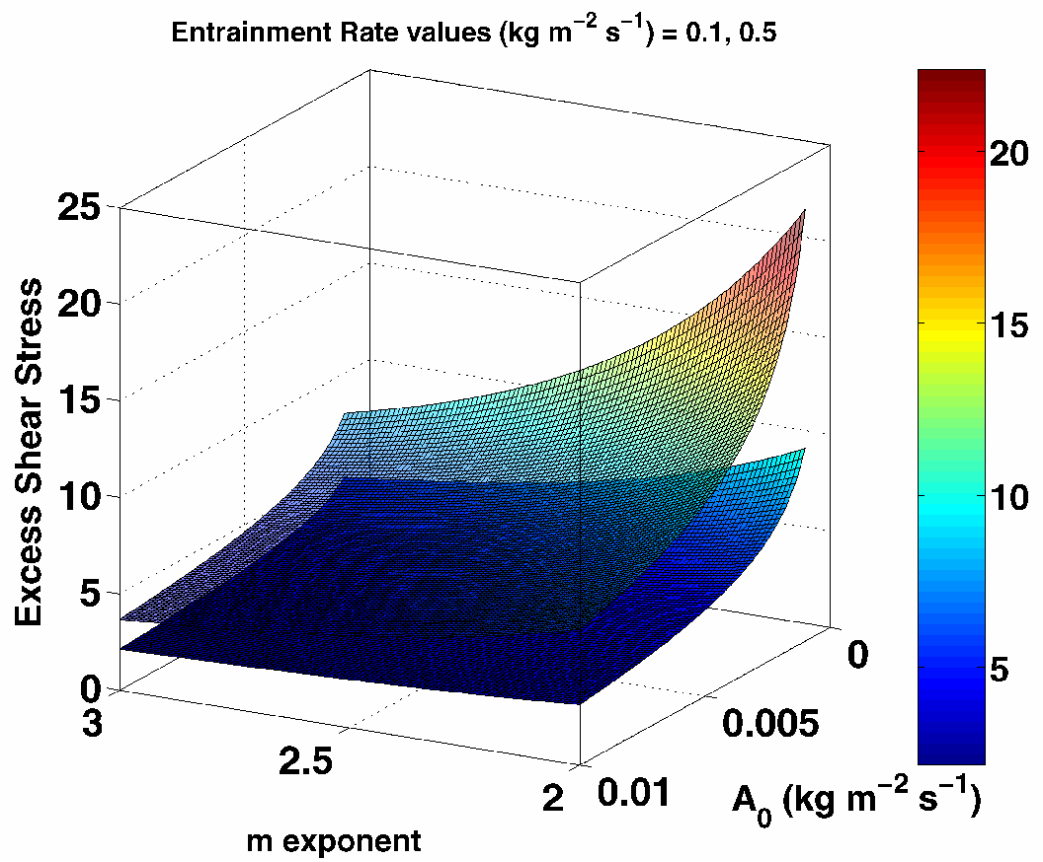

Figure 6. Isosurfaces of constant entrainment rate (E_B = 0.1, 0.5 kg m^{-2} s^{-1}) for a range of τ^*, A_0, and m. The colorbar represents the excess shear stress values.

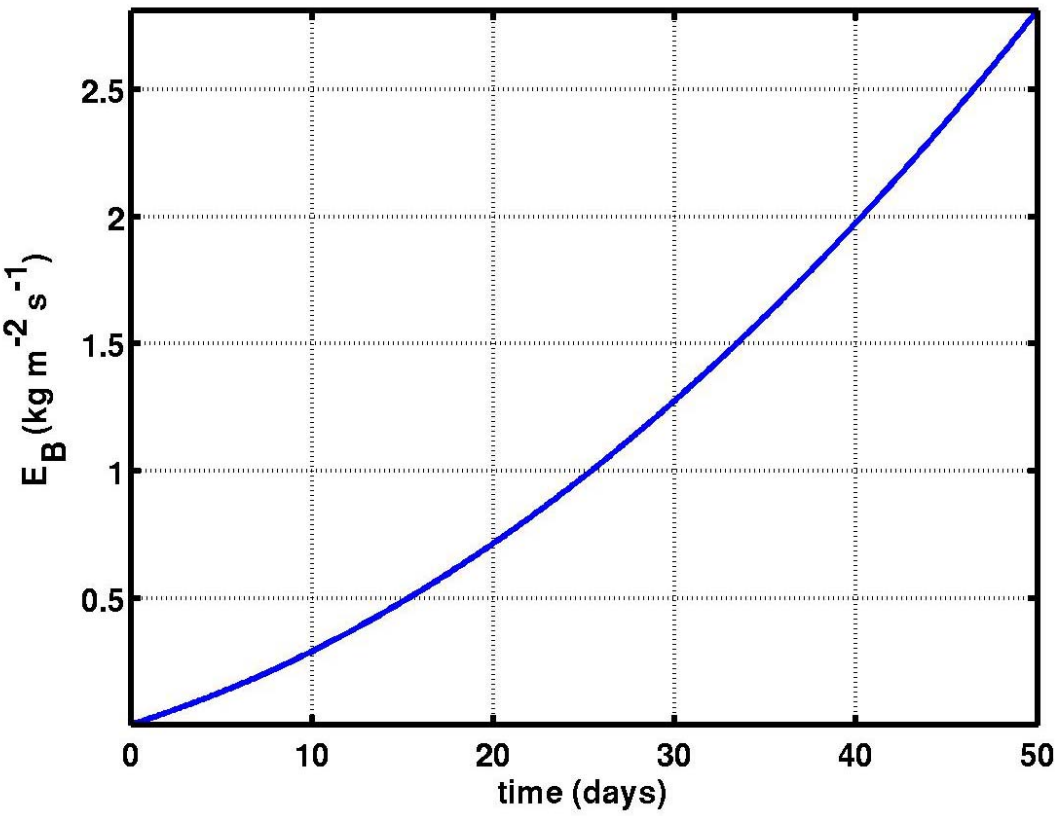

Figure 7. E_B (kg m^{-2} s^{-1}) as a function of deposition time (days). The parameters A_0 and τ^* are set equal to 1.0. The m exponent is set to zero.

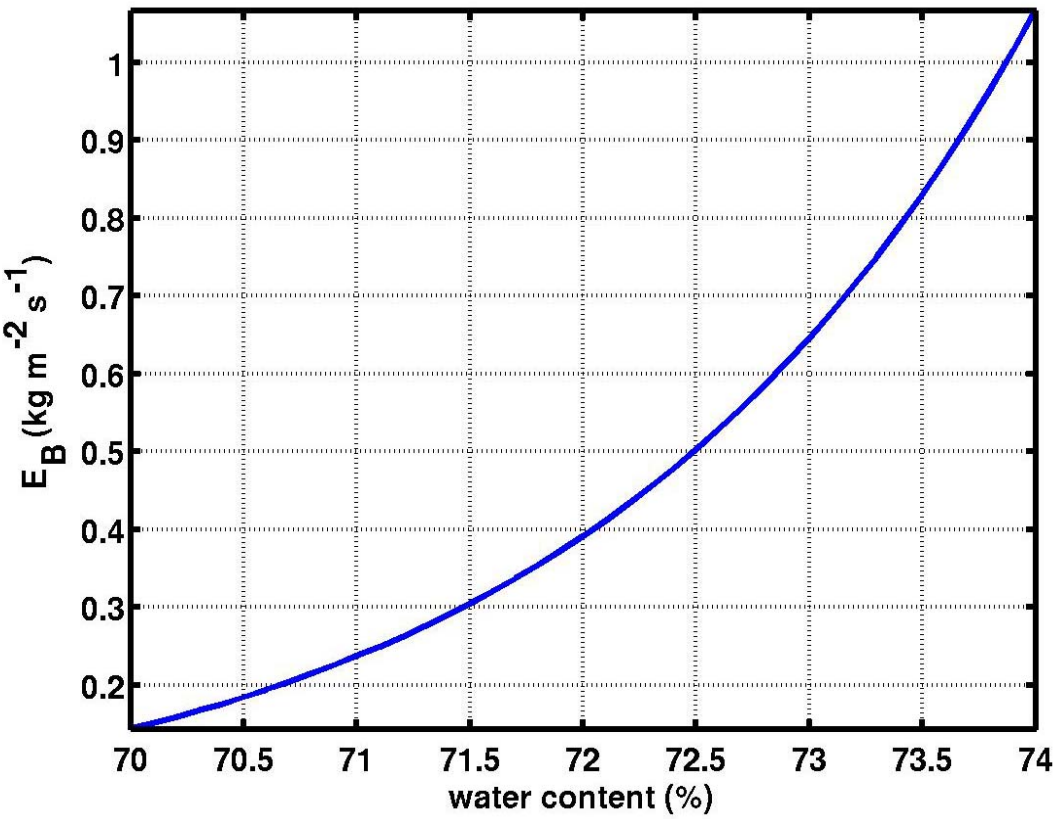

Figure 8. E_B (kg m^{-2} s^{-1}) as a function of water content (%). The parameters A_0 and τ* are set equal to 1.0. The *m* exponent is set to zero.

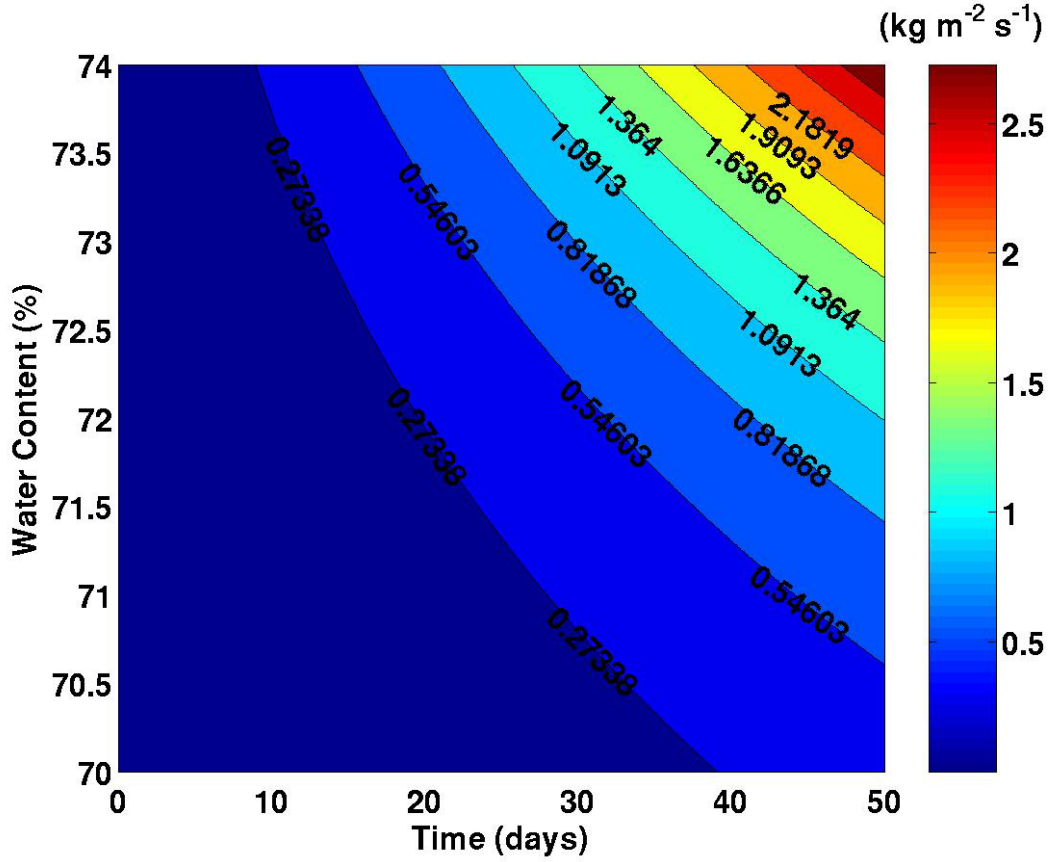

Figure 9. Contour plot of E_B (kg m^{-2} s^{-1}) as a function of deposition time (in days) and water content (%). The parameters A_0 and τ^* are set equal to 1.0. The m exponent is set to zero.

Figure 10. Entrainment rate (kg m^{-2} s^{-1}) curves with bioturbation or consolidation activated. A_0A_B is the factor for the dashed line and A_0A_C is the factor for the solid line. $A_0 = 0.001$ (kg m^{-2} s^{-1}) and the $m = 2.5$.

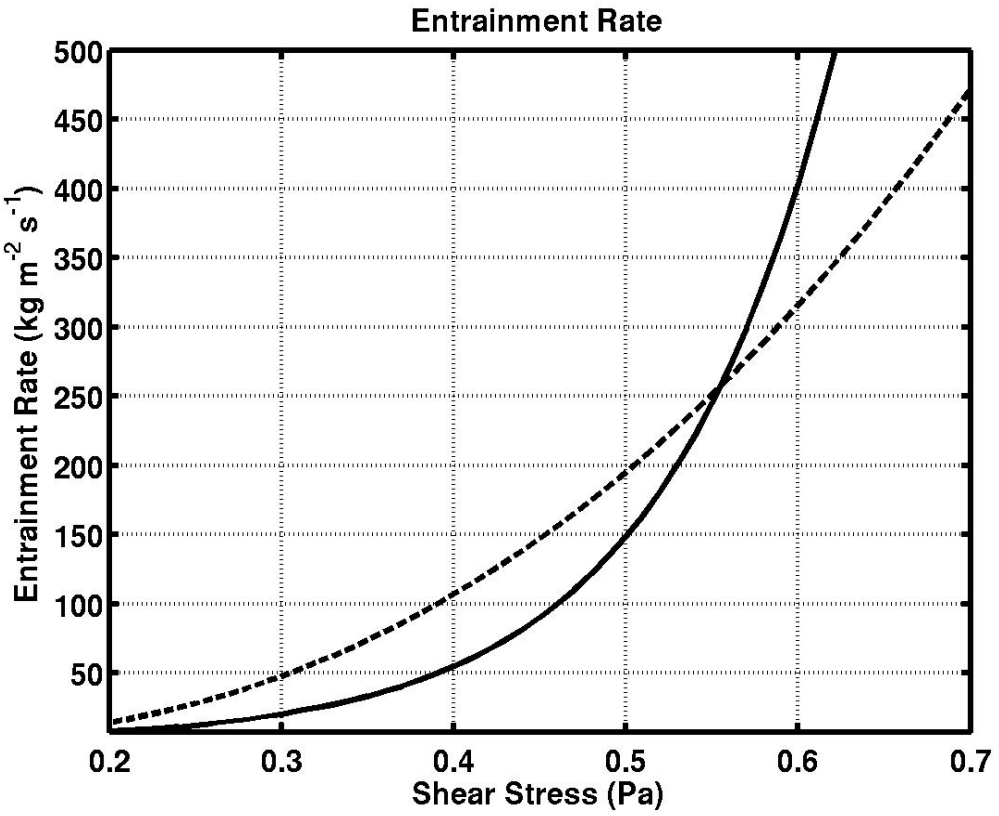

Figure 11. Power law and exponential entrainment rate (kg m^{-2} s^{-1}) functions vs. shear stress. The constant parameters of the power law function (dashed line) are A_0 = 1.0 kg m^{-2} s^{-1}, τ_c = 0.05 Pa, and m = 2.4. The constant parameters of the exponential function (solid line) are ε_0 = 1.0 kg m^{-2} s^{-1} and α = 0.1 Pa.